



Phase equilibria in the Cu–Fe–Ti system at 1123 K

J.A. van Beek, A.A. Kodentsov, F.J.J. van Loo*

Laboratory of Solid State Chemistry and Materials Science, TVM-CTK, P.O. Box 513, 5600 MB Eindhoven, Netherlands

Received 19 May 1994

Abstract

The isothermal cross-section through the ternary phase diagram Cu–Fe–Ti at 1123 K was constructed by means of a special diffusion technique developed earlier. The results have been verified on essential points by the investigation of equilibrated alloys. Five ternary intermetallic compounds designated as T_1 ($Ti_{33}Cu_{67-x}Fe_x$; $1 < x < 2.5$), T_2 ($Ti_{40}Cu_{60-x}Fe_x$; $5 < x < 17$), T_3 ($Ti_{43}Cu_{57-x}Fe_x$; $21 < x < 24$), τ ($Ti_{37}Cu_{63-x}Fe_x$; $6 < x < 7$) and τ_1 ($Ti_{45}Cu_{55-x}Fe_x$; $4 < x < 5$) exist as equilibrium phases in this system at 1123 K. Nearly 38 at.% Cu can be dissolved in cubic TiFe. This leads to an expansion of the lattice. It was found that at 1123 K the Cu-based solid solution is in equilibrium with intermetallic compounds of the binary Ti–Fe system and with the ternary phases T_2 and T_3 .

Keywords: Phase equilibria; Copper; Iron; Titanium

1. Introduction

Nowadays, Cu–Ag–Ti alloys are widely used as commercial active filler metals for joining various ceramics (Al_2O_3 , SiC, Si_3N_4) to iron-based alloys (steel). Knowledge about the quaternary phase diagram Cu–Ag–Ti–Fe is needed in order to predict the reaction products which are formed in the filler metal itself and at the interface with the Fe-based alloy during the brazing procedure and the further high temperature exposure of the joints.

The ternary systems Cu–Ag–Ti and Cu–Ag–Fe are already known quite satisfactorily [1–4]. However, no reliable experimental work has been reported on the Cu–Fe–Ti and Ag–Fe–Ti systems (phase equilibria in the Ag–Fe–Ti system at 1123 K will be discussed in a subsequent paper). Khan et al. [5] have studied the Cu-rich Cu–Fe–Ti alloys (up to 5 wt.% Ti and 5 wt.% Fe) in the temperature range 923–1173 K. They found that the equilibrium Cu–TiFe₂ exists in this system. Tekeuchi et al. [6] have reported on the partial liquidus projection in this system.

The isothermal cross-section through the ternary diagram Cu–Fe–Ti at 1123 K was constructed in the present work by combining a special diffusion technique

developed earlier [7] and the traditional methods of equilibrated alloys.

Anticipating the specific results of the present study, it seems worthwhile to make some general comments concerning the use of the diffusion technique in investigating ternary phase diagrams.

2. Determination of a ternary isothermal cross-section using diffusion methods

The idea to use diffusion couples for constructing multicomponent phase diagrams is based on the assumption of local equilibria in the diffusion zone. This implies that each infinitely thin layer of such a diffusion zone is in equilibrium with the neighbouring layers. In this case the sequence of the phases in the reaction zone and the distribution of the elements are determined by the phase diagram.

There are two variations of the diffusion method. In the first the sample to be studied is a classical semi-infinite diffusion couple, which means that after the diffusion annealing the couple ends still have their original compositions. If volume diffusion in such a system is the rate-limiting step, local equilibrium is supposed to exist and the rules which relate the composition of the diffusion zone to the phase diagram can be used [8] (Fig. 1). It is often necessary to investigate

*Corresponding author.

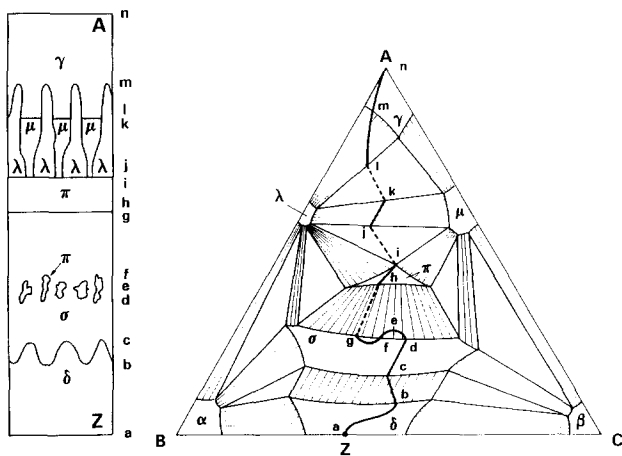


Fig. 1. The diffusion path in the reaction zone of a hypothetical couple A/Z plotted on the isotherm of the A–B–C phase diagram. The lower-case letters relate the structure to the appropriate composition on the isotherm.

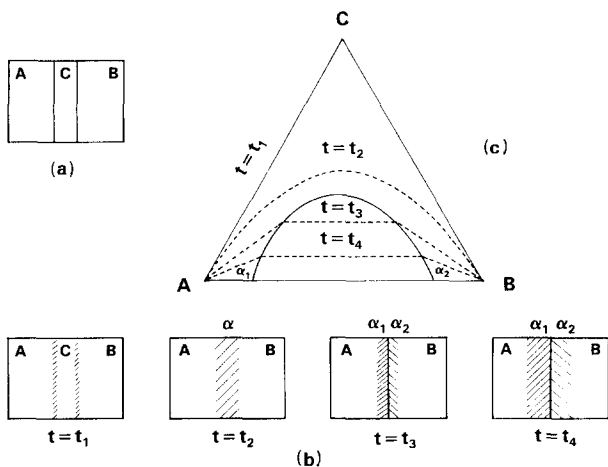


Fig. 2. Schematic view of reaction zones and diffusion paths on an isotherm after various annealing times: (a) initial sample; (b) morphology of the reaction zone for different annealing times; (c) diffusion paths for various annealing times.

couples with end members of various compositions in order to get all information needed to find the equilibrium data at the annealing temperature. The main feature of this method is that the phase composition of the reaction zone is independent of time and that the diffusion path (the composition–distance plot) is fixed.

Further development of the diffusion technique for constructing phase diagrams is connected with changing the macrostructure of the classical diffusion couple [7]. A sample is prepared by joining two plane-parallel slices of metal (alloy) through a thin layer of the third metal (alloy) (Fig. 2). In such a multilayered system the diffusion path is not fixed as in the classical diffusion couple. The phase composition of the complex diffusion zone is changing continuously with time as a result of the overlapping of two quasi-equilibrated diffusion zones. To relate the morphology and composition of

the reaction zone to the phase diagram rules similar to those for semi-infinite couples still can be used. For instance, the compositions found in the phases α_1 and α_2 at $t=t_3$ and t_4 respectively are the end points of two tie-lines in the two phase region.

3. Experimental details

Copper (99.99), iron (99.98) and titanium (99.98), supplied by Goodfellow (UK), were used as initial materials. The various Cu–Fe–Ti alloys were melted in an arc furnace under argon atmosphere using a non-consumable tungsten electrode. The ingots were remelted five times to improve their homogeneity. The weight loss of the alloys after melting was less than 1 wt.% relative. The specimens were annealed in an electroresistance furnace in evacuated quartz ampoules at 1123 K for 120–1500 h. The temperature was controlled within ± 3 K. After annealing the samples were quenched in water.

The ‘sandwich’ samples copper + titanium foil + iron and iron + copper foil + titanium were prepared and heat treated in vacuum (5×10^{-6} mbar) in an electron beam furnace, designed in our laboratory and described elsewhere [9]. The ‘sandwich’ couples were joined by an external load of 2 MPa.

After annealing and standard metallographic preparation, the ‘sandwich’ couples and alloys were examined by optical microscopy, scanning electron microscopy and electron probe microanalysis (EPMA). Because of the coarse structure of the annealed alloys, X-ray diffraction (XRD) analysis was performed with a cylindrical texture camera using nickel-filtered Cu $K\alpha$ or manganese-filtered Fe $K\alpha$ radiation [10].

4. Results

4.1. Interaction in the layered system Fe/Cu, foil (50 μm)/Ti at 1123 K

Microstructures of the reaction zone in the system Fe/Cu, foil (50 μm)/Ti after heat treatment at 1123 K for 24, 96 and 312 h are given in Fig. 3. Intermetallic compounds of the binary Ti–Cu system (Ti_2Cu , TiCu, Ti_3Cu_4 , Ti_2Cu_3 , TiCu_4) with very low iron content (less than 0.5 at.%) were found in the diffusion zone of the ‘sandwich’ sample mentioned above after annealing for 24 and 96 h. Besides that, the formation of a continuous layer of the ternary phase T_1 ($\text{Ti}_{33}\text{Cu}_{67-x}\text{Fe}_x$; $1 < x < 2.5$) between the layers Ti_2Cu_3 and TiCu_4 was observed. A layer of the copper-based solid solution (Cu_{ss}) was still detected within the diffusion zone after heat treatment of this sample even for 96 h (Fig. 3(b)). Further, the formation of a fragmented layer of another

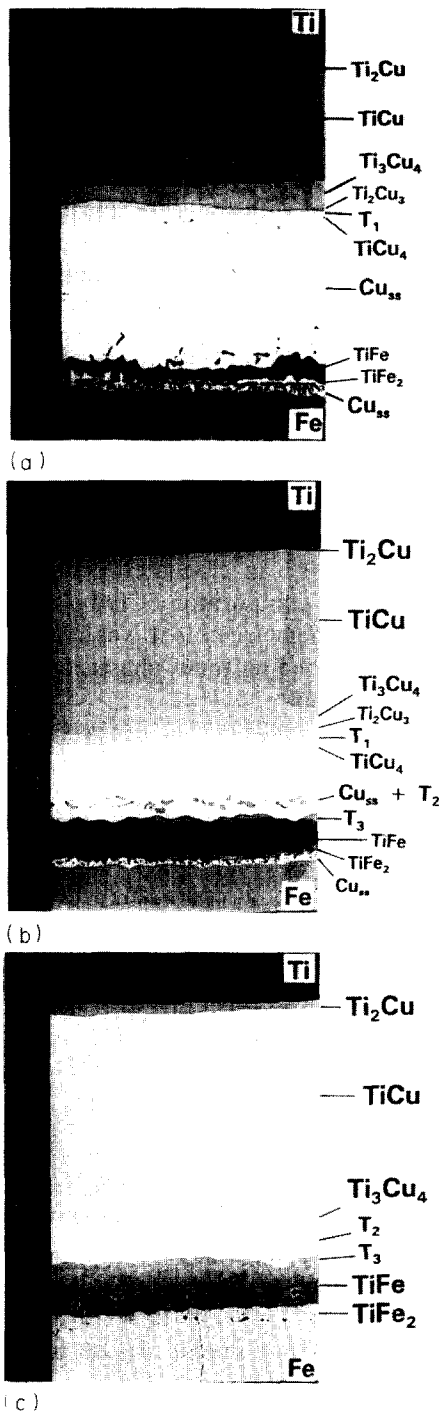


Fig. 3. Morphology of the reaction zone in the system Fe/Cu, foil (50 μm)/Ti after heat treatment at 1123 K for (a) 24 h, (b) 96 h and (c) 312 h.

ternary phase designated in the present work as T_3 ($Ti_{43}Cu_{57-x}Fe_x$; $21 < x < 24$) was clearly visible. This phase was found to be in equilibrium with TiFe and the Cu-based solid solution.

A characteristic feature of the reaction zones in the samples annealed for 24 and 96 h is the appearance of a layer of the Cu-based solid solution between $TiFe_2$ and the Fe-based solid solution (Fe_{ss}). This under-

lines the existence of the three-phase equilibrium $Fe_{ss} + Cu_{ss} + TiFe_2$ in the Cu–Fe–Ti system at this temperature. With increasing annealing time up to 312 h the layers of the Cu-based solid solution disappear completely and the ternary phase T_3 ($Ti_{43}Cu_{57-x}Fe_x$; $21 < x < 24$) was found in equilibrium with the ternary phase T_2 (Fig. 3(c)).

4.2. Interaction in the system Cu/Ti, foil/Fe at 1123 K

The morphology of the reaction zone in the ‘sandwich’ sample Cu/Ti, foil (100 μm)/Fe after annealing at 1123 K for 256 h is shown in Fig. 4.

A layer of β -Ti was still detected inside the diffusion zone. Nearly 15 at.% of iron and 5 at.% of copper were found in this layer. Close to the iron side of the reaction zone, layers of the intermetallic compounds $TiFe_2$ and $TiFe$ were formed. The concentration of copper in the $TiFe_2$ layer is less than 0.5 at.% while the layer of $TiFe$ contains about 4 at.% Cu.

From the copper side of the transition zone the sequence of layers of the intermetallic phases $TiCu_4$, Ti_2Cu_3 , Ti_3Cu_4 and $TiCu$ with very low Fe content (less than 0.5 at.%) was found. Deeper, however, the continuous layer of $TiCu$ contains isolated precipitates of $TiFe$ with nearly 38 at.% of copper. Then, the morphology of the two-phase region ($TiCu + TiFe$) changes and an interpenetrating columnar-type structure was observed. Columns of $TiCu$ (with less than 1 at.% Fe) are rooted in the adjoining $TiCu$ matrix whereas the irregular columns of $TiFe$ are also constituents of the next two-phase layer $Ti_2Cu + TiFe$ adjacent to the layer of β -Ti. The concentration of copper in $TiFe$ decreases within the two-phase layers towards the β -Ti side. The minimum Cu content in $TiFe$ in equilibrium with β -Ti was estimated as about 23 at.%.

For comparison we also annealed a ‘sandwich’ couple in which the Ti foil was 4 times as thin (25 μm) during

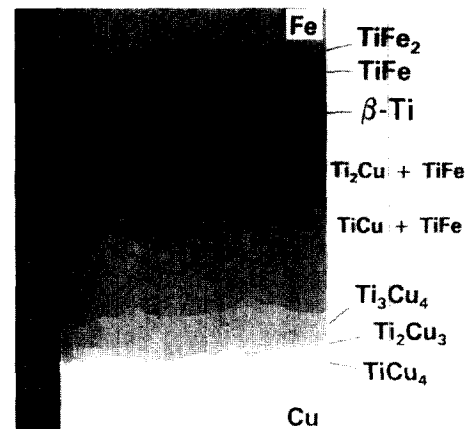


Fig. 4. Microstructure of the diffusion zone in the finite ‘sandwich’ sample Cu/Ti, foil (100 μm)/Fe after annealing at 1123 K for 256 h.

a time which was 16 times shorter (16 h). We expected to find, in principle, the same layer sequence according to the diffusion laws which predict a $t^{1/2}$ dependence of the layer thickness. However, no layer of β -Ti was found inside the reaction zone after annealing this 'sandwich' sample. Instead, a layer sequence TiFe_2 , TiFe , T_3 , T_2 and TiCu_4 was formed (Fig. 5(a)). A two-phase layer consisting of particles of TiCu_4 in the matrix of the ternary phase T_2 was observed within the diffusion zone. Towards the Cu side of the reaction zone, the morphology of this two-phase layer changed and precipitates of T_2 phase were visible inside the TiCu_4 matrix.

Only a continuous layer of TiFe_2 and a two-phase layer $\text{TiFe} + \text{Cu}_{ss}$ were detected after heat treatment of the same sample for 64 h (Fig. 5(b)). It can be seen from the micrograph that in some areas of the diffusion zone the particles of the Cu-based solid solution are in equilibrium with both intermetallic compounds of the Ti-Fe system (TiFe and TiFe_2). This proves the

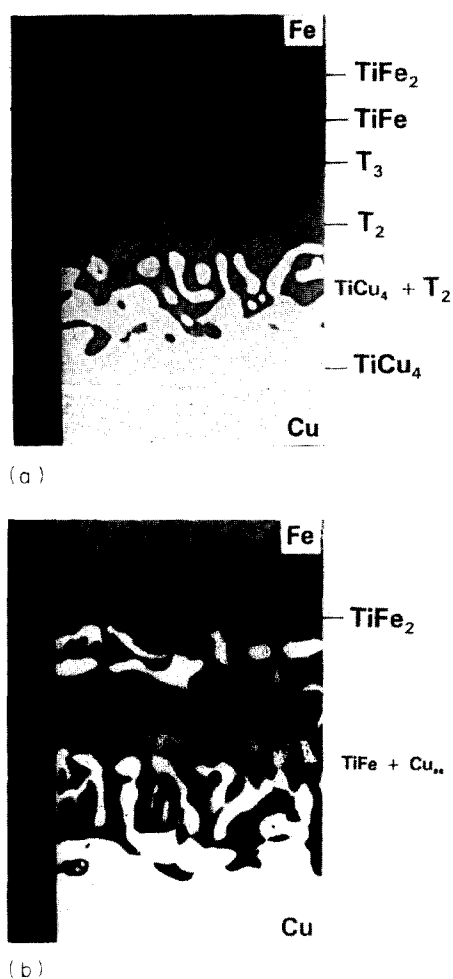


Fig. 5. Morphology of the reaction zone in the finite 'sandwich' sample Cu/Ti, foil (25 μm)/Fe after annealing at 1123 K for (a) 16 h and (b) 64 h.

presence of a three-phase equilibrium $\text{TiFe} + \text{TiFe}_2 + \text{Cu}_{ss}$ in the ternary Cu-Fe-Ti system at 1123 K.

From the morphology of the reaction layers in the diffusion zones of the 'sandwich' samples described above insight was gained into the possible phase equilibria in the Cu-Fe-Ti system at 1123 K. Moreover, information obtained with the diffusion technique was used as a guide for selecting the compositions of the alloys used to verify the provisionally found equilibria and to determine the boundaries of the phase fields in this ternary system.

4.3. Verification of the provisionally determined equilibria by investigating ternary equilibrated alloys

In Fig. 6 the microstructure of three-phase alloys studied in present work is shown after annealing at 1123 K for 120–1500 h in evacuated quartz ampoules and quenching. The composition of the phases present in the alloys after heat treatment was measured with EPMA and corresponding three-phase equilibria were plotted on the isotherm.

In order to determine more precisely the phase boundaries on this isotherm a number of two-phase alloys were examined with EPMA and XRD analysis. Results of this investigation are summarized in Table 1.

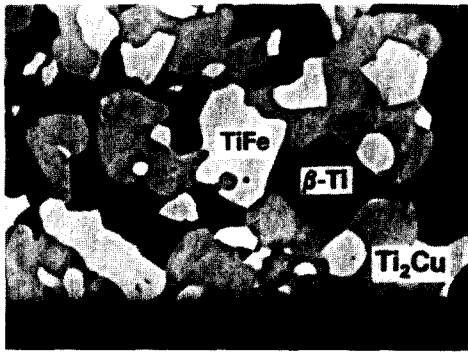
Finally, the results from phase analysis and equilibrium concentration measurements in 'sandwich' samples and equilibrated alloys led to the cross-section of the Cu-Fe-Ti diagram at 1123 K represented in Fig. 7.

5. Discussion

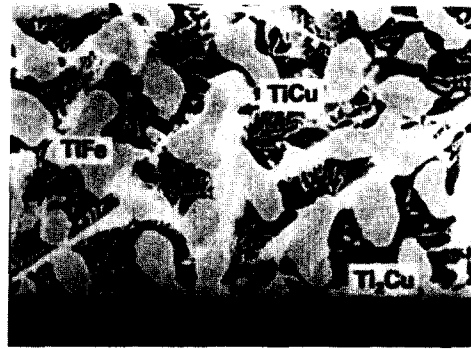
A conspicuous feature of the Cu-Fe-Ti system at 1123 K is the formation of a number of ternary phases, designated as T_1 , T_2 , T_3 , τ and τ_1 . Phase T_1 ($\text{Ti}_{33}\text{Cu}_{67-x}\text{Fe}_x$; $1 < x < 2.5$) exists as an equilibrium phase in this system at 1123 K. In the corresponding binary Ti-Cu the phase TiCu_2 is not stable in its pure form at 1123 K and can only be formed by the peritectic reaction $\text{Ti}_3\text{Cu}_4 + \text{L} \rightleftharpoons \text{TiCu}_2$ at higher temperature 1163 ± 10 K [11]. Probably, a small amount of iron (about 1 at.%) stabilizes TiCu_2 , thus resembling the stabilization of TiCu_2 by the substitution of Cu by Ni atoms in the case of the Cu-Ni-Ti system [12].

The homogeneity region of the Ti_2Cu phase extends to about 2 at.% Fe in the ternary Cu-Fe-Ti system. The existence of a Ti_2Fe compound has been mentioned previously [13], but this turned out to be a phase stabilized by an impurity component such as oxygen or nitrogen [14].

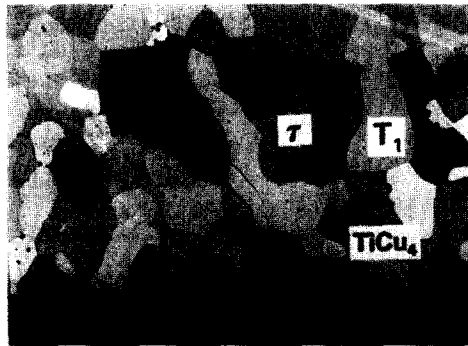
The structure of the phases T_2 and T_3 was found to be closely related to that of Ti_2Cu_3 ($P4/nmm$) and Ti_3Cu_4 ($I4/mmm$) respectively. Phase T_2 was found to



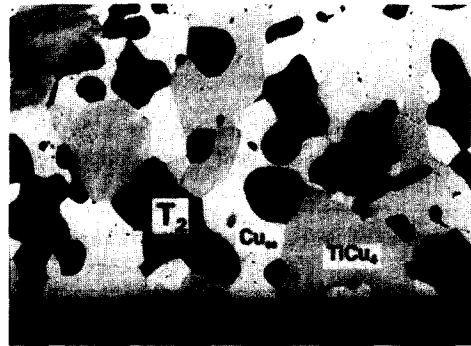
(a)



(b)



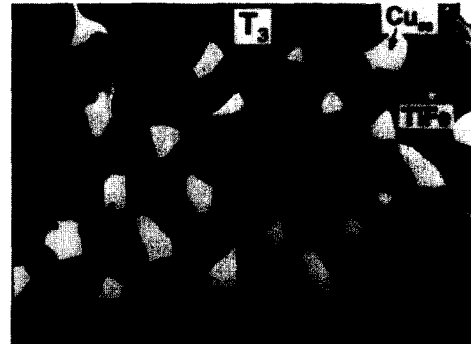
(c)



(d)



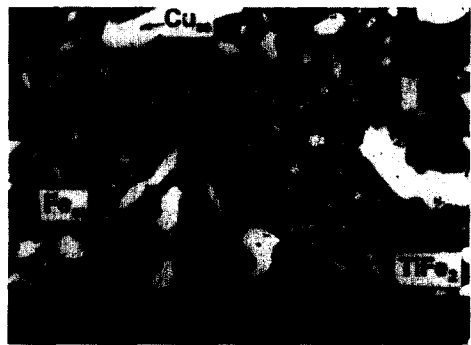
(e)



(f)



(g)



(h)

Fig. 6.

(continued)

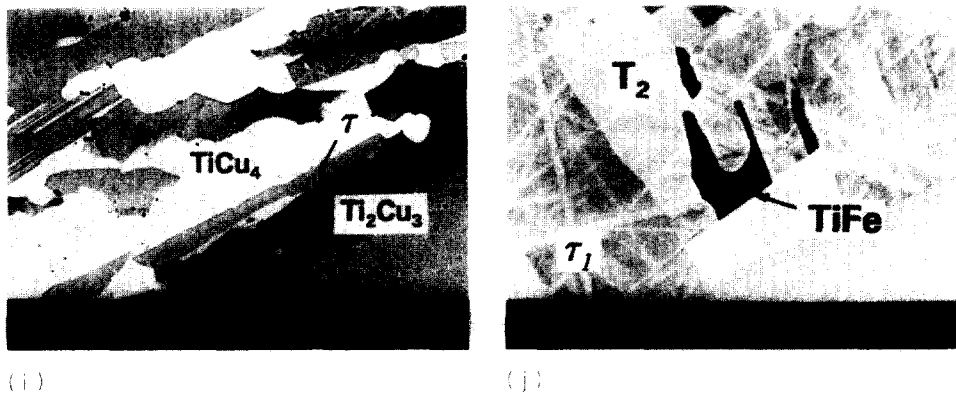


Fig. 6. Microstructures of three-phase alloys in the Cu–Fe–Ti system after annealing at 1123 K for 120–1500 h (backscattered electron images): (a) $\text{Cu}_{20}\text{Fe}_{15}\text{Ti}_{65}$; (b) $\text{Cu}_{40}\text{Fe}_5\text{Ti}_{55}$; (c) $\text{Cu}_{60}\text{Fe}_5\text{Ti}_{35}$; (d) $\text{Cu}_{70}\text{Fe}_5\text{Ti}_{25}$; (e) $\text{Cu}_{45}\text{Fe}_{18}\text{Ti}_{37}$; (f) $\text{Cu}_{37}\text{Fe}_{25}\text{Ti}_{38}$; (g) $\text{Cu}_{30}\text{Fe}_{25}\text{Ti}_{35}$; (h) $\text{Cu}_{30}\text{Fe}_{60}\text{Ti}_{10}$; (i) $\text{Cu}_{60}\text{Fe}_5\text{Ti}_{35}$; (j) $\text{Cu}_{48}\text{Fe}_8\text{Ti}_{44}$. (The various phases on the micrographs are denoted by their binary formulae).

Table 1

Phases present in equilibrated alloys after annealing at 1123 K according to electron probe microanalysis and X-ray diffraction analysis^a

Alloy	Annealing time (h)	Phases present at 1123 K
$\text{Cu}_{15}\text{Fe}_{60}\text{Ti}_{25}$	768	$\text{TiFe}_2 + \text{Cu}_{ss}$
$\text{Cu}_{30}\text{Fe}_{30}\text{Ti}_{40}$	480	$\text{TiFe} + \text{Cu}_{ss}$
$\text{Cu}_8\text{Fe}_{25}\text{Ti}_{67}$	480	$\text{TiFe} + \beta\text{-Ti}$
$\text{Cu}_{15}\text{Fe}_{25}\text{Ti}_{60}$	624	$\text{TiFe} + \beta\text{-Ti}$
$\text{Cu}_5\text{Fe}_{35}\text{Ti}_{60}$	624	$\text{TiFe} + \beta\text{-Ti}$
$\text{Cu}_{35}\text{Fe}_{10}\text{Ti}_{55}$	120	$\text{TiFe} + \text{Ti}_2\text{Cu}$
$\text{Cu}_{30}\text{Fe}_{15}\text{Ti}_{55}$	672	$\text{TiFe} + \text{Ti}_2\text{Cu}$
$\text{Cu}_{15}\text{Fe}_5\text{Ti}_{80}$	624	$\text{Ti}_2\text{Cu} + \beta\text{-Ti}$
$\text{Cu}_{21}\text{Fe}_{30}\text{Ti}_{49}$	480	$\text{TiFe} + \text{T}_3$
$\text{Cu}_{33}\text{Fe}_{20}\text{Ti}_{47}$	672	$\text{TiFe} + \text{T}_2$
$\text{Cu}_{54}\text{Fe}_{16}\text{Ti}_{30}$	480	$\text{Cu}_{ss} + \text{T}_3$
$\text{Cu}_{53}\text{Fe}_{10}\text{Ti}_{37}$	504	$\text{TiCu}_4 + \text{T}_2$
$\text{Cu}_{54}\text{Fe}_5\text{Ti}_{41}$	1464	$\text{Ti}_3\text{Cu}_4 + \text{T}_2$
$\text{Cu}_{54}\text{Fe}_7\text{Ti}_{39}$	768	$\text{T}_2 + \tau$
$\text{Cu}_{40}\text{Fe}_{13}\text{Ti}_{47}$	768	$\text{TiFe} + \text{T}_2$
$\text{Cu}_{41}\text{Fe}_{18}\text{Ti}_{41}$	480	$\text{T}_2 + \text{T}_3$
$\text{Cu}_{43}\text{Fe}_9\text{Ti}_{48}$	672	$\text{TiFe} + \tau_1$

^aThe various phases are denoted by their binary formulae.

be stable between about 5 and about 17 at.% of Fe and the ternary phase T_3 exists at this temperature at higher Fe content (from about 21 to about 24 at.%). It is possible that the T_2 phase is continuous with the phase Ti_2Cu_3 from the binary Ti–Cu system, containing up to about 17 at.% Fe at this temperature. However, the ternary phases τ ($\text{Ti}_{37}\text{Cu}_{63-x}\text{Fe}_x$; $5 < x < 7$) and τ_1 with a very narrow region of homogeneity (composition of this phase was determined as $\text{Ti}_{45}\text{Cu}_{55-x}\text{Fe}_x$; $4 < x < 5$) have no isostructural compounds in binary Ti–Cu system.

Another characteristic feature of this isotherm is a large solubility of Cu in the intermetallic compound TiFe (up to 38 at.%) which was expected based on the comparison of the Cu–Fe–Ti system with the Ni–Fe–Ti and Cu–Ni–Ti isotherms (at 1143 K and 1173

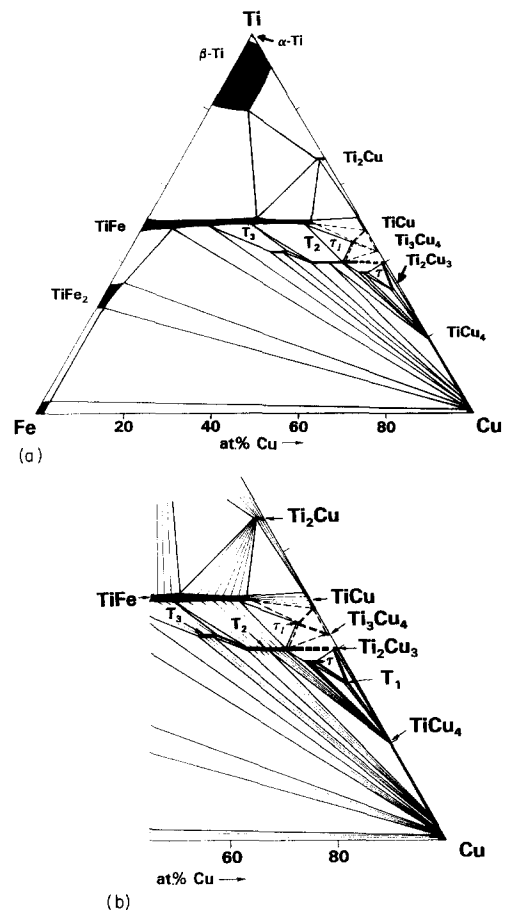


Fig. 7. Isothermal cross-section through the ternary phase diagram Cu–Fe–Ti at 1123 K determined in the present study: (a) general view; (b) magnified Cu-rich region of the diagram.

K respectively) determined earlier [12,14]. Substitution of Fe by Cu atoms leads to an expansion of the cubic lattice of TiFe. A similar behaviour was found in the case of substitution of Ni by Cu atoms in the cubic lattice of TiNi (TiNi and TiFe are miscible at this temperature completely).

A narrow region of α -Ti still exists in this ternary system at 1123 K, but the presence of iron and copper stabilizes the b.c.c. structure of β -Ti.

6. Concluding remarks

It is very important to realize that a number of error sources might appear when multiphase diffusion experiments are used for constructing phase diagram [7,15]. The difficulties connected with the accurate determination of the boundary concentrations are a problem for both semi-infinite (classical) and finite diffusion couples techniques. Steep concentration gradients sometimes occur in growing layers in the reaction zone. To estimate the boundary concentrations an extrapolation is then necessary which might lead to quite large errors. Moreover, accurate electron microprobe measurements near the interface are sometimes very difficult owing to fluorescence effects [16].

Another group of problems arises from the formation of the quasi-equilibrated diffusion zone.

(1) Impurities present in the starting materials may play a large role. Segregation of impurities (especially O, N, C) can cause an enrichment in the diffusion zone and the diffusion path might miss an equilibrium phase. On the contrary, the same effect can cause the formation of phases, stabilized by impurities.

(2) Metastable equilibria can be established in the diffusion zone, especially at the initial stages of the interaction. Again, some phases present at the equilibrium isotherm can be missed. This can also be caused by a slow growth rate (low diffusion coefficients) of the missing phase.

Unquestionably, the diffusion technique used in the present study has large advantages. The efficiency of this method is very high. By making only one finite 'sandwich' sample, reannealed and investigated various times, much information can be gained about the whole isotherm.

However, in order to increase the reliability of the information obtained about the ternary isotherm a

combination of the diffusion methods with an investigation of selected equilibrated alloys is desirable.

Acknowledgements

We wish to thank Mr. P. Broers for designing and operating the vacuum furnaces which play an important role in this research project.

The investigation was supported by the Netherlands Foundation for Chemical Research (SON) with financial aid from the Netherlands Organization for Scientific Research (NWO).

References

- [1] V.N. Eremenko, Yu.I. Buyanov and N.M. Panchenko, *Izv. Akad. Nauk SSSR Metall.*, 3 (1969) 188.
- [2] V.N. Eremenko, Yu.I. Buyanov and N.M. Panchenko, *Izv. Akad. Nauk SSSR Metall.*, 5 (1969) 299.
- [3] W. Hume-Rothery and R.A. Buckley, *J. Iron Steel Inst.*, 202 (1964) 531.
- [4] A.A. Bochvor, A.S. Ekatova, E.V. Panchenko and Yu.F. Sidokhin, *Dokl. Akad. Nauk SSSR*, 174 (1967) 863.
- [5] M.G. Khan, A.M. Zakharov and M.V. Zakharov, *Izv. Vyssh. Uchebn. Zaved., Tsvetn. Metall.*, 1 (1970) 104.
- [6] Y. Takeuchi, M. Watanabe and S. Yamabe, *Metall.*, 22 (1968) 8.
- [7] E.M. Slusarenko, S.F. Dunaev, E.M. Sokolovskaya and A.A. Kodentsov, in *Phase Diagrams in Physical Metallurgy*, Naukova Dumka, Kiev, 1984, p. 73.
- [8] J.B. Clark, *Trans. Metall. Soc. AIME*, 227 (1963) 1250.
- [9] W. Wakelkamp, *Ph.D. Thesis*, Eindhoven University of Technology, 1991.
- [10] C.A. Wallace and R.C.C. Ward, *J. Appl. Crystallogr.*, 8 (1975) 2555.
- [11] Th.B. Massalski, in *Binary Alloy Phase Diagrams II*, ASM, Metals Park, OH, 1986.
- [12] F.J.J. van Loo, G.F. Bastin and A.J.H. Leenen, *J. Less-Common Met.*, 57 (1978) 111.
- [13] M. Hansen, in *Constitution of Binary Alloys*, McGraw-Hill, New York, 1958.
- [14] F.J.J. van Loo, J.W.G.A. Vrolijk and G.F. Bastin, *J. Less-Common Met.*, 77 (1981) 121.
- [15] F.J.J. van Loo, *Prog. Solid State Chem.*, 20 (1990) 47.
- [16] G.F. Bastin, F.J.J. van Loo, P.J.C. Vosters and J.W.G.A. Vrolijk, *Scanning*, 5 (1983) 172.